

Chiral-symmetry breaking and light-quark masses in lattice QCD

Herbert W. Hamber

The Institute for Advanced Study, Princeton, New Jersey 08540

(Received 2 July 1984)

The chiral order parameter and the masses of the pseudoscalar and vector mesons are computed in lattice QCD neglecting fermion-polarization effects on lattices of size up to $8 \times 8 \times 8 \times 16$. Five values of the gauge coupling constants are considered and the results are compared with the weak-coupling asymptotic-freedom predictions. Estimates for the values of the light-quark masses are presented and their scaling behavior is studied. A preliminary study of the spatial-size dependence of physical quantities is presented. Finite-size scaling methods are used to compare the results for the vector-pseudoscalar-meson spin splittings on the larger lattice with results on a $4 \times 4 \times 4 \times 16$ and $6 \times 6 \times 6 \times 12$ lattice. This allows one to penetrate deeper in the weak-coupling region. Around $g^2=1$ the results would suggest significant deviations from two-loop asymptotic-freedom scaling.

I. INTRODUCTION

Lattice gauge theory presents a well defined framework in which nonperturbative calculations in QCD can be performed from first principles.^{1,2} This represents a qualitatively novel situation compared to phenomenological approaches that have been used with varying degrees of success in the past.

Recent attempts to compute the hadron spectrum by numerical methods were necessarily limited to rather small lattices and relatively large lattice spacings, and the natural question arises of what is the relationship of these results to the expected continuum physics at weak coupling, where asymptotic freedom makes definite predictions about the scaling properties of physical quantities. Furthermore in most studies an approximation was used in which the fermion-polarization effects were neglected, and the question of chiral-symmetry restoration at weak coupling still needs to be clarified.³

In principle the dependence of physical quantities on the cutoffs can be investigated by increasing the lattice size and by reducing the gauge coupling, assuming one has statistical systematic effects under control, and by varying the form of the lattice action so as to reduce the effects of irrelevant operators.^{2,4}

In a previous work some results were presented for the fermion condensate $\langle \bar{\psi}\psi \rangle$ (Ref. 5) and the mass of the lowest-lying meson states^{5,6} as obtained on a lattice of size $6 \times 6 \times 6 \times 12$. We used there the Kogut-Susskind form of the fermion action since it presents some advantages because of its chiral properties. The dependence of the results on the size of the box was not investigated and for the masses the study was basically restricted to only one value of the gauge coupling constant ($g^2=1$). Even though the results appeared reasonable, the belief that they had relevance for the continuum limit of the theory was based on the assumption that the onset of "scaling" for the string tension [at about $g^2=1.09$ for SU(3)] was appearing also in the light-hadron masses at about the same value of the coupling. This conclusion was also supported by the fact that the scaling for $\langle \bar{\psi}\psi \rangle$ appeared to

be quite convincing.

In this paper we continue the study of chiral-symmetry breaking and the light-hadron masses by investigating the size and coupling-constant dependence of the results. As in our previous studies, we neglect for simplicity the effects of internal fermion loops. In Sec. II we introduce our notational and discuss the size dependence of $\langle \bar{\psi}\psi \rangle$. On an $8 \times 8 \times 8 \times 8$ lattice five values for the gauge coupling constant ($\beta=6/g^2=5.6, 5.7, 5.8, 5.9, 6.0$) were studied and for each coupling the quark mass was varied over six different values ($m=0.30, 0.25, 0.20, 0.15, 0.10, 0.05$). The results show small size dependences for quark masses that are greater than 0.05 and the values obtained by extrapolating to zero mass are consistent with previous determinations.

In Sec. III we present our results for the pseudoscalar- and vector-meson masses on an $8 \times 8 \times 8 \times 16$ lattice. The behavior of $\langle \bar{\psi}\psi \rangle$ and the vector-meson mass extrapolated to zero-quark mass appears to be consistent with scaling in the range of coupling investigated. The pion decay constant also shows scaling behavior, but its value is always somewhat the experimental value. The information on the slope of the pseudoscalar-meson mass squared versus the quark mass is then used to extract the values of the light-quark masses for each value of g^2 . For the values of coupling constant investigated we also find that the ratio between the pseudoscalar mass squared and the quark mass in lattice units appears to start to scale later than the previous quantities. Nevertheless, it appears that some physical quantities such as ratios of masses tend to remain constant (within our errors) in the "crossover" region. On the other hand, no scaling behavior is found for the first radial excitation of the pseudoscalar meson, a situation which we attribute to the larger statistical and systematic errors in this case.

In Sec. IV we address the important question of the relevance of our results to the continuum limit. A real-space renormalization-group transformation is constructed by comparing the results for the ρ mass on the $8 \times 8 \times 8 \times 16$ lattice with results on a $4 \times 4 \times 4 \times 16$ lattice. The procedure is similar in spirit to the finite-size scaling

method: for weak enough coupling a change in the size of the lattice can be compensated by a shift in the coupling β to give the same ρ mass in lattice units. The amount of the shift is predicted for weak-enough coupling by the two-loop β function. If on the finite lattice a shift in the gauge coupling is found which is consistent with the perturbative prediction, then this can be taken as an indication of matching to the weak-coupling regime. Our preliminary results seem to indicate that such a matching does indeed take place not too far beyond $\beta=6$. In Sec. V we then present our conclusions.

II. CHIRAL-SYMMETRY BREAKING

Let us first introduce our notation. The pure gauge part of the theory is defined in terms of a set of gauge matrices $U_{n\mu}$ that reside on the links of the lattice and are elements of the group SU(3):

$$S_G = \frac{\beta}{6} \sum_{n,\mu < \nu} \text{Tr} U_{n,\mu} U_{n+\mu,\nu} U_{n+\nu,\mu}^\dagger U_{n,\nu}^\dagger + \text{c.c.}, \quad (2.1)$$

where we have set $\beta=6/g^2$. The lattice fermion action is^{2,7}

$$S_F = -\frac{1}{2} \sum_f \sum_{n,\mu} [\bar{\psi}_{n+\mu}^{(f)}(r-\gamma_\mu) U_{n\mu}^\dagger \psi_n^{(f)} + \bar{\psi}_n^{(f)}(r+\gamma_\mu) U_{n\mu} \psi_{n+\mu}^{(f)}] + (m+4r) \sum_f \sum_n \bar{\psi}_n^{(f)} \psi_n^{(f)}. \quad (2.2)$$

The γ 's are Euclidean γ matrices and obey $\{\gamma_\mu, \gamma_\nu\} = 2\delta_{\mu\nu}$ and $\gamma_\mu^\dagger = \gamma_\mu$. We also have set for simplicity the lattice spacing $a=1$. In this paper we will study exclusively the fermion action with $\gamma=0$ ("naive action"),^{1,8} since we are interested in the chiral properties of the theory, which are somewhat mutilated for nonzero γ . Also, we will restrict the number of fermion flavors n_f to one. The action of Eq. (2.2) is known to describe 16 fermions in the continuum. We prefer to write the fermion action in the Susskind form⁸ and reduce the number of fermion flavors from 16 to 4. The spin diagonalization can be achieved by making the unitary transformation⁷

$$\psi_n = T_n \chi_n, \quad \bar{\psi}_n = \bar{\chi}_n T_n^\dagger, \quad T_n = \gamma_1^{n_1} \gamma_2^{n_2} \gamma_3^{n_3} \gamma_4^{n_4}. \quad (2.3)$$

As a result one obtains a sum of four identical actions, each of the form

$$S_F = \frac{1}{2} \sum_{n,\mu} \eta_{n,\mu} (\bar{\chi}_{n+\mu} U_{n\mu}^\dagger \chi_n - \bar{\chi}_n U_{n,\mu} \chi_{n+\mu}) - m \sum_n \bar{\chi}_n \chi_n \quad (2.4)$$

with $\eta_{n,\mu} = (-1)^{n_1 + \dots + n_{\mu-1}}$, and χ can now be taken to be a one-component Fermi field.

The above action describes $4n_f$ (instead of $16n_f$) fermion flavors, and has a continuous $U(n) \times U(n)$ chiral symmetry when the mass parameter m is set to zero.^{7,9,10} Here n is the number of noncolor indices of the χ fermion field. These symmetries correspond to baryon-number and flavor-nonsinglet-charge conservation, respectively, and it is the second one that is spontaneously broken both

at strong and at intermediate coupling. Note that these symmetries are *not* the same as the $U(4) \times U(4)$ chiral symmetry of a continuum action with four flavors. Still, an important consequence of the residual chiral symmetry is that no mass counterterms are generated when the gauge-field interaction is included and no parameters need to be adjusted to obtain a massless pion.

In the new action formulated in terms of the χ fields only the *even* sites should be identified with the points in the physical Euclidean space, and the four Dirac fields should be thought of as constructed out of the 16 χ fields in the unit cell of size $2a$. This circumstance and the presence of four flavors gives rise to factors of 2 when comparing lattice with continuum quantities such as

$$a^{-3} \frac{1}{V} \sum_n \langle \bar{\chi}_n \chi_n \rangle = 4 \langle \bar{\psi} \psi \rangle_{\text{cont, 1flavor}}. \quad (2.5)$$

Unless otherwise stated, in the following we will refer, when quoting specific numbers in the tables and in the graphs, to $\langle \psi \psi \rangle$ as the quantity corresponding to *two* flavors in the continuum. In the lattice theory one is interested in evaluating expectation values of gauge-invariant operators. In order to do this, the relevant operators have to be averaged over the gauge and fermion variables. The quantum expectation value of a physical observable $O(U, \psi, \bar{\psi})$ is given by

$$\langle O \rangle = Z^{-1} \int [dU][d\bar{\psi}][d\psi] O(U, \psi, \bar{\psi}) e^{S_G + S_F}. \quad (2.6)$$

Here

$$[dU] = \prod_n dU_n$$

is the invariant measure on SU(3), and the fermion integration means

$$[d\bar{\psi}][d\psi] = \prod_{n,\alpha,\alpha'} d\bar{\psi}_{\alpha n}^{a(f)} \prod_{m,\beta,\beta'} d\psi_{\beta m}^{b(f')}. \quad (2.7)$$

Z is the partition function

$$Z = \int [dU][d\bar{\psi}][d\psi] e^{S_G + S_F}. \quad (2.7)$$

For weak-enough coupling physical quantities like hadron masses are expected to scale according to the asymptotic-freedom prediction and thus become proportional to the QCD scale parameter

$$\Lambda_{\text{latt}} = \frac{1}{a} (\beta_0 g^2)^{\beta_1/2\beta_0^2} e^{-1/2\beta_0 g^2 + O(g^2)}. \quad (2.8)$$

In the following, fermion-polarization effects will be neglected ($n_f=0$), and then one has for the group SU(3)

$$\beta_0 = \frac{11}{16\pi^2}, \quad \beta_1 = \frac{51}{128\pi^4}. \quad (2.9)$$

A quantity of interest is the condensate wave function $\langle \bar{\psi} \psi \rangle$ (Refs. 5 and 11), and it is given by

$$\langle \bar{\psi}_n \psi_n \rangle = Z^{-1} \int [dU] \Delta^{-1} [U]_{n,n} e^{S_G[U]}, \quad (2.10)$$

and Δ^{-1} is the inverse of the matrix that defines the fermion action in Eq. (2.2). It is only meaningful to calculate its value for the $\gamma=0$ action, since otherwise the

chiral symmetry is explicitly broken and the above quantity cannot be used to define an order parameter because of perturbative contributions. In the free-fermion theory $\langle \bar{\psi}\psi \rangle$ vanishes when the quark mass is reduced to zero. A nonvanishing result in the interacting theory in the same limit signals spontaneous breaking of chiral symmetry and the ensuing existence of Goldstone modes. A spectral representation for $\langle \bar{\psi}\psi \rangle$ can be written

$$\langle \bar{\psi}\psi \rangle = \frac{m}{V} \int d\lambda \frac{\rho(\lambda)}{\lambda^2 + m^2}. \quad (2.11)$$

For free fermions $\rho(\lambda)$ behaves like λ^3 for small λ . Dynamical chiral-symmetry breaking implies a nonvanishing spectral density at low frequency:

$$\lim_{m \rightarrow 0} \langle \bar{\psi}\psi \rangle = \frac{\pi}{V} \rho(0). \quad (2.12)$$

In practice $\langle \bar{\psi}\psi \rangle$ is computed on a finite lattice (with periodic boundary conditions) and, before averaging, on a given background-gauge-field configuration, using stochastic methods like the Monte Carlo method or the Langevin equation for fermions (relaxation methods are impractical for this quantity).^{5,11,12}

It is a well-known result that no spontaneous symmetry breaking can occur on a finite lattice, and thus $\langle \bar{\psi}\psi \rangle$ has to ultimately vanish in the interacting theory when the quark mass is reduced to zero. A signal for spontaneous symmetry breaking is when a nonzero order parameter is found when the volume is sent to infinity *first*, and *then* the external field (in this case the mass) is sent to zero. Therefore it is only the volume-independent part of the order parameter that is of relevance for the discussion on symmetry breaking:

$$\langle \bar{\psi}\psi \rangle = \lim_{m \rightarrow 0} \lim_{V \rightarrow \infty} \frac{1}{V} \sum_n \langle \bar{\psi}_n \psi_n \rangle_{m, V}. \quad (2.13)$$

The schematic behavior of $\langle \bar{\psi}\psi \rangle$ on a finite lattice as a function of m is shown in Fig. 1. Its purpose is to show that it is the *envelope* of the finite-lattice curves that is of

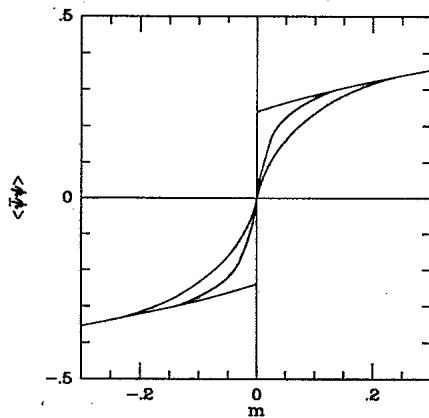


FIG. 1. Qualitative behavior of the order parameter $\langle \bar{\psi}\psi \rangle$ as a function of the quark mass m . On a finite lattice it tends to zero for small quark mass. In the infinite-volume limit the region in which size dependence is observed shrinks to zero, and the size independent part of $\langle \bar{\psi}\psi \rangle$ (the envelope of the finite lattice curves) develops a discontinuity at $m = 0$.

TABLE I. $\langle \bar{\psi}\psi \rangle$ on a $6 \times 6 \times 6 \times 6$ lattice (the data is taken from Ref. 5). The last column contains the extrapolated value at $m = 0$.

$\beta \backslash m$	0.30	0.25	0.20	0.15	0.10	0.00
5.0	0.684	0.679	0.681	0.653	0.627	0.56
5.1	0.674	0.656	0.643	0.645	0.589	0.52
5.2	0.659	0.638	0.628	0.614	0.564	0.48
5.3	0.631	0.622	0.598	0.573	0.534	0.46
5.4	0.621	0.606	0.576	0.540	0.539	0.43
5.5	0.588	0.560	0.542	0.498	0.481	0.40
5.6	0.539	0.502	0.473	0.427	0.392	0.30
5.7	0.516	0.490	0.440	0.401	0.335	0.20
5.8	0.498	0.440	0.398	0.368	0.280	0.15
5.9	0.469	0.431	0.373	0.330	0.233	0.06
6.0	0.468	0.429	0.379	0.319	0.232	0.05
6.1	0.449	0.401	0.353	0.285	0.219	0.04
6.2	0.436	0.395	0.340	0.271	0.190	0.01
6.3	0.427	0.383	0.326	0.273	0.180	0.00

interest in the continuum limit. The rest are lattice artifacts. Also we notice that for negative m the sign of $\langle \bar{\psi}\psi \rangle$ should be flipped.

In Ref. 5, $\langle \bar{\psi}\psi \rangle$ was computed on a $6 \times 6 \times 6 \times 6$ lattice for several values of m and β and gauge group SU(3).

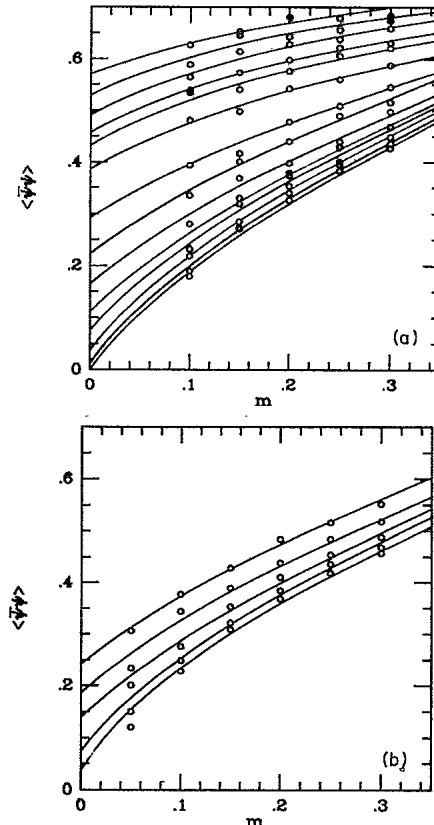


FIG. 2. (a) The quantity $\langle \bar{\psi}\psi \rangle$ for two flavors on the $6 \times 6 \times 6 \times 6$ lattice as a function of the quark mass m for different values of β (see Table I). The curves are only intended as a guide to the eye. (b) The quantity $\langle \bar{\psi}\psi \rangle$ for two flavors on the $8 \times 8 \times 8 \times 8$ lattice as a function of the quark mass m for different values of β (see Table II). The curves are only intended as a guide to the eye.

TABLE II. $\langle\bar{\psi}\psi\rangle$ on an $8\times 8\times 8\times 8$ lattice. The second column also lists the values of the average plaquette. The last two columns contain the extrapolated values at $m=0$ obtained using the point at $m=0.05$ in the quadratic-polynomial fit and discarding it because of possible finite-size effects, respectively.

β	$1-\langle\text{Tr}U_p\rangle/N$	m							
		0.30	0.25	0.20	0.15	0.10	0.05	0.00	
5.6	0.4752	0.552	0.516	0.484	0.428	0.377	0.306	0.232	0.242
5.7	0.4502	0.518	0.484	0.438	0.389	0.344	0.234	0.150	0.232
5.8	0.4320	0.488	0.454	0.410	0.353	0.276	0.201	0.105	0.087
5.9	0.4181	0.468	0.436	0.384	0.322	0.249	0.150	0.045	0.059
6.0	0.4061	0.457	0.418	0.368	0.309	0.228	0.121	0.009	0.036

There the gauge coupling constant was chosen to lie inside the narrow (in the coupling constant) crossover region ($5.5 \leq \beta \leq 6.2$, with $\beta=6/g^2$), where approximate scaling behavior for the string tension^{13,14} is observed.

The values for $\langle\bar{\psi}\psi\rangle$ for this lattice are presented in Table I and in graphic form in Fig. 2(a). We have repeated in part the calculation on a slightly larger lattice ($8\times 8\times 8\times 8$) to estimate the importance of finite-size effects. For 5 values of β and 6 values of m we have computed $\langle\bar{\psi}\psi\rangle$ on 2–4 configurations averaging over 200–600 fermion sweeps. For each value of β and m the configurations were chosen to be statistically independent. In the computation we used the Langevin equation, and discarded the results from the first 100 iterations. We have preferred this technique over the Monte Carlo method because of its faster convergence rate for this particular quantity. At each value of (β, m) we used a different statistically independent gauge-field configuration, separated from the previous one by 100 iterations if at the same value of β and 300 if the value of β differed. We also averaged over configurations obtained from hot and cold starts. For three values of (β, m) we have checked our results with the Monte Carlo method. At each value of β, m we have also computed $\langle\bar{\psi}\psi\rangle$ using the relaxation method on an $8\times 8\times 8\times 16$ lattice for a few (2–6) lattice points for both periodic and open boundary conditions in the time direction obtaining again results consistent with the other determinations within the errors. More details on the general aspects of the techniques used can be found in Ref. 3, and references therein.

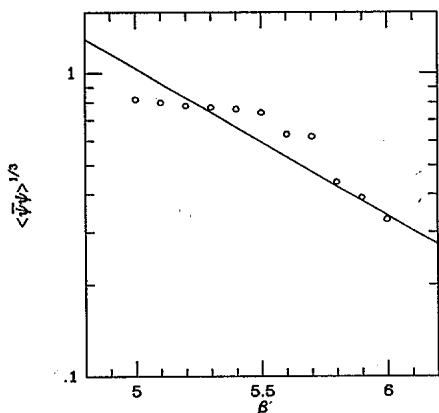


FIG. 3. $\langle\bar{\psi}\psi\rangle$ at $m=0$ as a function of β . The expected renormalization-group behavior is also shown. The straight line represents the estimate $\langle\bar{\psi}\psi\rangle=(110\pm 15)^3(2\beta_0g^2)^{-4/11}\Lambda_{\text{latt}}^3$.

The results on the larger lattice are displayed in Table II and Fig. 2(b). As can be seen from comparing the two sets of quantities the finite-size effects are rather small up to $m=0.1$. For $m=0.05$ the values on the larger lattice are slightly below the extrapolated value obtained from the smaller lattice, indicating that they might not be trusted in an extrapolation. Also, the size dependence appears to be larger for weaker coupling. A least-squares quadratic-polynomial fit to the remaining points then gives the extrapolated values at $m=0$, listed in the last column of Table II.

If chiral symmetry is spontaneously broken, then for weak-enough coupling one expects $\langle\bar{\psi}\psi\rangle$ to scale as Λ^3 times an anomalous dimension factor. In Fig. 3 we show its behavior as a function of β . It appears that the scaling is quite convincing, and from the graph we estimate

$$\langle\bar{\psi}\psi\rangle=R^3(2\beta_0g^2)^{-4/11}\Lambda_{\text{latt}}^3 \quad (2.14)$$

with $R=110\pm 15$. On the other hand, we notice that for weaker coupling there is a tendency for R to become smaller. At $\beta=5.6, 5.7, 5.8, 5.9$, and 6.0 we find $R=135, 150, 120, 115$, and 110 , respectively, so that a value for R as low as 90 for weaker coupling cannot be excluded. A study with higher statistics on a larger lattice should clarify this issue. It should be kept in mind that perturbative corrections affect Λ and that the peak that is observed in the specific heat at $\beta\approx 5.55$ could lead to some distortion in the results. We will return to this question later on. If we use the value for the lattice spacing obtained in the next section from the ρ mass for each value of β and take the average, we obtain the estimate for two flavors $\langle\bar{\psi}\psi\rangle 2\times(460\pm 60 \text{ MeV})^3$ in the region $g^2\approx 1$.

III. MASSES OF LIGHT MESONS AND QUARKS

Let us now turn to a discussion of the light-hadron spectrum. The way by which the masses and decay constants are extracted from the lattice propagators has been extensively discussed before in the literature (see, for example, again Ref. 3, and references therein). Here we will only recall the main results and formulas that are relevant for the following discussion.

The masses of the lighter hadrons can be obtained by computing the appropriate fermion correlation functions of composite operators. In the case we are interested in, these are given for the mesons by the formulas

$$\begin{aligned} \langle \bar{\psi}\psi(x)\bar{\psi}\psi(0) \rangle_{I \neq 0} &= \int d\mu[U] \text{Tr} [\Delta^{-1}(x,0|U)\Delta^{-1}(0,x|U)], \\ \langle \bar{\psi}\psi(x)\bar{\psi}\psi(0) \rangle_{I=0} &= \int d\mu[U] \text{Tr} [\Delta^{-1}(x,0|U)\Delta^{-1}(0,x|U)] - n_f \int d\mu[U] \text{Tr} [\Delta^{-1}(x,x|U)\Delta^{-1}(0,0|U)], \end{aligned} \quad (3.1)$$

and for the baryons

$$\langle \bar{\psi}\bar{\psi}\bar{\psi}(x)\psi\psi\psi(0) \rangle = \int d\mu[U] \text{Tr} [\Delta^{-1}(x,0|U)\Delta^{-1}(x,0|U)\Delta^{-1}(x,0|U)], \quad (3.2)$$

where we have suppressed color and spinor indices for simplicity. We have set

$$d\mu[U] = Z^{-1} \exp(S) d[U],$$

and Δ is the lattice Dirac operator as defined through the action of Eq. (2.2). With $I=0$ we denote here a flavor singlet, and assume that the flavor symmetry is unbroken. In the following discussions we will restrict ourselves to the pseudoscalar- and vector-meson states. Results for some of the heavier mesons and the baryons for the Susskind action will be presented elsewhere.

Let us call the propagator for a given (meson or baryon) state $G(x)$. Then it is convenient to have states with zero spatial momentum propagate in time, which can be achieved by looking at the propagator summed over spatial coordinates. From the large-distance behavior of the propagators the masses are then determined through their exponential falloff

$$\tilde{G}_\Gamma(t) = \sum_x G_\Gamma(x) \underset{t \rightarrow \infty}{\sim} A e^{-m_\Gamma t}. \quad (3.3)$$

At intermediate separation other states $|n\rangle$ which are higher in mass and have the same quantum numbers as the operator $\bar{\psi}\Gamma\psi$ tend to contribute. A Lehmann representation for the propagator shows that

$$\tilde{G}_\Gamma(t) = \sum_n |\langle 0 | \bar{\psi}(0)\Gamma\psi(0) | n \rangle|^2 e^{-m_n t}, \quad (3.4)$$

and the intermediate states $|n\rangle$ above the first excited state are the radial recurrences. The amplitudes of the exponentials are also of physical relevance since they are related to the decay constants.

The spin-parity assignments in the case of the Kogut-Susskind fermions are not so straightforward, because states of different spin-parity can contribute to the same correlation function.^{5,6,10,11} In order to extract the masses one first considers the meson propagator

$$G_M(x) = \sum_{ab} |\Delta_{ab}^{-1}(x)|^2 \quad (3.5)$$

and the baryon propagator

$$G_B(x) = \sum_{abc} \sum_{a'b'c'} \epsilon^{abc} \epsilon^{a'b'c'} \Delta_{aa'}^{-1}(x) \Delta_{bb'}^{-1}(x) \Delta_{cc'}^{-1}(x). \quad (3.6)$$

In order to separate the states with different spin-parity it is convenient to consider the four kinds of corners of the spatial Brillouin zone. One defines

$$\begin{aligned} G_M^0(t) &= \sum_x G_M(x), \\ G_M^1(t) &= \sum_x [(-1)^x + (-1)^y + (-1)^z] G_M(x), \\ G_M^2(t) &= \sum_x [(-1)^{x+y} + (-1)^{y+z} + (-1)^{z+x}] G_M(x), \\ G_M^3(t) &= \sum_x (-1)^{x+y+z} G_M(x). \end{aligned} \quad (3.7)$$

It is then easy to prove that for large t the above propagators behave like

$$\begin{aligned} G_M^0(t) &\underset{t \rightarrow \infty}{\sim} e^{-m_P t}, \\ G_M^1(t) &\underset{t \rightarrow \infty}{\sim} e^{-m_V t} + (-1)^t e^{-m_A t}, \\ G_M^2(t) &\underset{t \rightarrow \infty}{\sim} e^{-m_V t} + (-1)^t e^{-m_A t}, \\ G_M^3(t) &\underset{t \rightarrow \infty}{\sim} e^{-m_P t} + (-1)^t e^{-m_S t}, \end{aligned} \quad (3.8)$$

where P , V , S , A , and T stand for pseudoscalar, vector, scalar, axial vector, and tensor. It is clear that in the case of the staggered fermions the analysis of the correlation functions is made more difficult by the presence of more than one particle.

In the case of the baryons similar projections on the Brillouin boundary can be done. It turns out that also in this case states of different parity contribute to the same correlation function (one finds that, when the mass of the baryon is not small in lattice units, the states that propagate forward and backward are mixtures of spin $\frac{1}{2}^+$ and $\frac{1}{2}^-$ states).¹⁰

On the lattice one is of course interested in eventually approaching the chiral limit $m_q \rightarrow 0$. Because of long relaxation times for small quark masses and the finite box size, the range of quark masses typically accessible in the crossover region is between $m_q a = 0.3$ and $m_q a = 0.02$, corresponding to a physical quark mass which can be at most reduced to about 50 MeV, an order of magnitude still above the physical m_u, m_d quark masses.

Statistical and systematic errors tend to affect the computation of the masses. Statistical fluctuations in the gauge-field configurations contribute to the statistical errors in the masses. The higher the relative mass of the state, the higher in general the fluctuation.

The masses of the hadrons are obtained in practice by fitting the correlation functions to the expected exponential or hyperbolic cosine (or sum thereof). At short distances ($t \ll m^{-1}$) the correlation functions follow in general power-law behavior, while at larger separation a contamination from higher excitations (the radial recurrences)

TABLE III. Some results for $\langle\bar{\psi}\psi\rangle$ and the pseudoscalar and vector masses in lattice units as a function of the quark mass m on a $4\times 4\times 4\times 16$ lattice at $g^2=\infty$. The column with $m=0$ contains the approximate extrapolated values, and the last column contains the exact values at $m=0$ and $g^2N=\infty$ from Refs. 7, 9, and 10, listed for comparison.

m	0.30	0.20	0.10	0.00	Exact
$\langle\bar{\psi}\psi\rangle$	0.91	0.93	0.96	0.98	$3\frac{\sqrt{7}}{8}=0.992$
m_P	1.17	0.94	0.67	0	0
m_V	1.97	1.93	1.88	1.82	$\cosh^{-1}3=1.763$
m_P^2/m	4.55	4.45	4.52	4.51	$\frac{12}{\sqrt{7}}=4.536$

will be present. One notices in general that for smaller quark masses and weaker gauge coupling the expected asymptotic behavior sets in more slowly. This is the reason why one chooses to work on an asymmetric lattice: by making the lattices longer in the "time" direction these effects can be reduced. Of course the higher the separation, the larger the statistical errors will be and more statistical accuracy is needed. This is the first source of systematic errors.

The physical region of small quark masses has to be, at least with the presently available lattice sizes, obtained by extrapolation using the values of the masses computed for larger quark masses. The finite spatial extent of the lattice poses a limit on the smallest pion mass that can be reached: the inverse pion mass in lattice units should be at most about one half the size of the lattice. This is equivalent to the requirement that the pion wave function should fit inside the box (and the size of the wave function goes like the inverse of the mass of the state). Also, for pion masses greater than about 0.2–0.1 in lattice units the cutoff-dependent corrections to the fermion propagator are significant, as can be seen comparing the hadron mass values for $\gamma=0$ and $\gamma=1$ using the same quark mass as input. Another way of phrasing these requirements is that the masses in lattice units should lie between the ultraviolet and the infrared lattice cutoff: $\pi/La \ll m \ll \pi/a$, and m can be made small only if L , the spatial extent of the box, is made large. An improved fermion action could make the extrapolation problem less acute. This is the second source of systematic errors.

The physical masses of the hadrons are obtained then by extrapolating the results obtained at finite coupling to the limit of zero coupling using the renormalization group. In order to do this one has to check that the results at finite coupling scale in accordance with the predictions of asymptotic freedom. The glue correlation length (the inverse glueball mass) grows very rapidly in this region, and one cannot make the coupling too small because of boundary effects. In other words, on a finite lattice both the quarks and the gluons can wind around the periodic lattice if they are light enough, giving rise to unphysical results. In a box of finite volume it is easy to show that the size effects are exponential in the mass gap times the linear size of the box. Because of machine-time limitation it is often possible to study only a few (1–3) values of the gauge coupling constant in the crossover region. One then hopes that in this region one is close

enough to the asymptotic behavior, since for the masses the corrections are of order $\Lambda^2 a^2$. In the case of the decay constants, perturbative corrections proportional to g^2 are in general present. For the pion decay constants obtained using the local operator one finds, for example,¹⁵

$$f_\pi^{\text{cont}} = [1 - 0.12g^2 + O(g^4)] f_\pi^{\text{latt}}. \quad (3.9)$$

This is the third source of systematic effects.

As a first test of our methods we have computed the pseudoscalar and vector mass and $\langle\bar{\psi}\psi\rangle$ on a $4\times 4\times 4\times 16$ lattice at $\beta=0$. The results can be used as a check and are displayed in Table III together with the exact answers from Refs. 7, 9, and 10. As can be seen, at least in this regime the numerical results even on such a small lattice are in good agreement (within a few percent) with the analytic ones.

In Table IV we have listed for later comparison some of the results obtained in Ref. 6 on a $6\times 6\times 6\times 12$ lattice at $\beta=6.0$. For finite β our results for the pseudoscalar and vector masses on an $8\times 8\times 8\times 16$ lattice are shown in Tables V and VI. The pseudoscalar mass was obtained from the analysis of the first propagator of Eq. (3.7) and the vector-meson mass from the second propagator in the same equation. The other two propagators were also analyzed and gave comparable results, but with larger statistical errors. As usual the masses were obtained fitting the propagators to a sum of two hyperbolic cosines, with the one or two points close to the origin removed in the fit. Because of the number of points used, the fit tends to be rather reliable and does not depend significantly on whether the points at separation 0 and 1 are included or not. Typically we have found that the two-hyperbolic-cosine fit gives values for the mass estimates for fixed β and m that are about five percent lower than the t (time-

TABLE IV. Pseudoscalar-meson mass, vector-meson mass, pseudoscalar decay constant, and first radial excitation of the pseudoscalar in lattice units as a function of m at $\beta=6.0$ as obtained on a $6\times 6\times 6\times 12$ lattice (from Ref. 6).

m	0.30	0.20	0.10	0.00
m_P	1.21	0.94	0.60	0
m_V	1.35	1.10	0.77	0.51
f_P	0.23	0.19	0.16	0.12
m_P	1.57	1.32	1.04	0.78

TABLE V. Pseudoscalar-meson masses in lattice units as a function of β and m as obtained on the $8 \times 8 \times 8 \times 16$ lattice. The numbers in parentheses indicate the error.

$m \backslash \beta$	0.30	0.25	0.20	0.15	0.10	0.05
5.6	1.32(1)	1.20(1)	1.09(2)	0.95(2)	0.77(3)	0.55(1)
5.7	1.31(2)	1.20(1)	1.08(3)	0.94(2)	0.76(3)	0.53(5)
5.8	1.30(1)	1.19(1)	1.08(1)	0.93(2)	0.75(5)	0.52(6)
5.9	1.27(4)	1.17(4)	1.04(3)	0.89(2)	0.72(5)	0.48(3)
6.0	1.20(1)	1.09(5)	0.95(8)	0.82(4)	0.62(3)	0.41(2)

slice)-dependent mass estimates $m(t) = \ln G(t-1)/G(t)$. These tend to be slowly convergent even in the case of Kogut-Susskind fermions, where the asymptotic regime of pure exponential decay seems to be reached significantly faster (for comparable values of the pion mass) than in the Wilson fermion case. For the smaller values of the quark mass ($m < 0.2$) we have also checked our results by using open boundary conditions for the fermions in the time directions, and found agreement within the errors. Non-periodic boundary conditions have the disadvantage of giving rise to larger statistical noise and no average can be taken over the forward and backward propagation as in the periodic case. Also it is not always clear in the case of nonperiodic boundary conditions at what separation one should stop because of possible boundary effects.

The mass of the vector meson at $m=0$ for each β was obtained by linearly extrapolating the mass-squared difference $m_V^2 - m_P^2$, which is slowly varying as a function of m in the data, and is almost constant experimentally when going from the ρ to the J/ψ . We also include in Tables VII and VIII estimates for the pseudoscalar decay constant and the mass of the first radial excitation in the pseudoscalar channel. The results were obtained by computing the propagators on two independent gauge configurations for $m > 0.15$ and on four independent configurations for the smaller values of m . The fermion propagators were computed using the relaxation method with 100–400 iterations and convergence was checked by evaluating the quantity

$$\langle \bar{\psi}\psi \rangle - 4m \int dt G_\pi(t), \quad (3.10)$$

which is zero configuration by configuration for any m and on a finite lattice because of chiral symmetry, if the propagator is evaluated exactly, and was kept in the present computation smaller than 10^{-5} . Since a different configuration was used for each value of m , separated from the preceding one by 100 Monte Carlo iterations (with 10 hits), the values of the masses and other param-

eters can be thought of as independent for different values of both m and β .

As can be seen from Table V and Fig. 4(a), due to the large size of the lattice the statistical errors are rather small and can be estimated at a few percent. In general there is a trend for the masses and the spin splittings to slightly decrease as the number of configurations is increased, but we estimate that this effect is included in our errors. We also estimate that the systematic errors due to the finite extent of the box in the time direction are comparable or smaller than the statistical errors, because of the length 16 employed. We will postpone until later a discussion of the finite-size effects due to the finite box size in the spatial direction. In Table IV we also list for comparison the analogous estimates for the masses and decay constants obtained in Ref. 6 on a $6 \times 6 \times 6 \times 12$ lattice. The results appear to be consistent with each other within the errors.

From the table and the graphs it appears that we have good control over the pseudoscalar mass, and the noise is, not unexpectedly, significantly larger for the vector-meson mass. Let us discuss the behavior of the pseudoscalar mass and its dependence on the quark mass first. Current algebra predicts that in the continuum the pseudoscalar mass squared is linear in the quark mass,

$$2M_\pi^2 f_\pi^2 = \langle \bar{\psi}_u \psi_u + \bar{\psi}_d \psi_d \rangle (m_u + m_d) + O(m^2 \ln m^2), \quad (3.11)$$

and we will not consider here for simplicity the case of unequal quark masses. It is easy to prove that this identity is satisfied *exactly* on the lattice for all couplings in the limit of small quark mass. It follows from the definition of f_π ,

$$(m_u + m_d) \langle 0 | \bar{\psi}_u \gamma_5 \psi_d | \pi \rangle = \sqrt{2} f_\pi m_\pi^2, \quad (3.12)$$

which implies for the pion propagator at large distances

TABLE VI. Vector-meson masses in lattice units as a function of β and m as obtained on the $8 \times 8 \times 8 \times 16$ lattice. The numbers in parentheses indicate the error.

$m \backslash \beta$	0.30	0.25	0.20	0.15	0.10	0.05	0.00
5.6	1.67(5)	1.56(7)	1.44(5)	1.29(9)	1.15(8)	0.96(11)	0.78
5.7	1.65(7)	1.54(8)	1.42(9)	1.26(4)	1.12(3)	0.95(9)	0.75
5.8	1.62(5)	1.52(3)	1.40(3)	1.24(9)	1.06(6)	0.86(12)	0.63
5.9	1.48(7)	1.40(2)	1.28(13)	1.08(3)	0.98(6)	0.73(3)	0.54
6.0	1.39(6)	1.28(9)	1.14(7)	0.95(4)	0.81(4)	0.62(9)	0.45

TABLE VII. Pseudoscalar-meson decay constant in lattice units as a function of β and m obtained on the $8 \times 8 \times 8 \times 16$ lattice. The numbers in parentheses indicate the error.

$\beta \backslash m$	0.30	0.25	0.20	0.15	0.10	0.05	0.00
5.6	0.41(2)	0.37(2)	0.33(2)	0.30(3)	0.24(2)	0.20(2)	0.18
5.7	0.37(3)	0.34(2)	0.28(1)	0.25(3)	0.21(3)	0.17(3)	0.16
5.8	0.34(1)	0.30(1)	0.27(2)	0.21(2)	0.20(4)	0.15(2)	0.14
5.9	0.30(2)	0.27(1)	0.24(2)	0.20(2)	0.17(2)	0.14(2)	0.11
6.0	0.27(1)	0.23(1)	0.21(2)	0.18(3)	0.16(1)	0.11(1)	0.09

$$G_{\pi}(t) \underset{t \rightarrow \infty}{\sim} \frac{f_{\pi}^2 m_{\pi}^3}{4m^2} e^{-m_{\pi} t}, \quad (3.13)$$

and from the exact sum rule for $G_{\pi}(t)$, evaluated for small m_{π} .

As can be seen from Fig. 4(a) for the smaller values of β the pseudoscalar mass squared is remarkably linear in the quark mass, in fact it is difficult to detect at $\beta=5.6$ and 5.7 any deviation from linearity in the range of quark masses we have investigated. For larger β 's (5.9 and 6.0) some curvature sets in at the smaller mass values. This is not unexpected since in the continuum the ratio M_P^2/m should scale as Λ , up to an anomalous dimension factor. What is nevertheless surprising is that scaling for this ratio sets in (if it sets in at all) at a value of β (≈ 5.9) that is significantly after the region where there is a peak in the specific heat and the crossover phenomenon in the string tension is observed ($\beta \approx 5.55$). In Fig. 4(b) the analogous

results for the vector-meson mass are presented.

In order to compute the light-quark masses an evaluation of the lattice spacing is needed, which we chose to extract from the ρ mass. The sum of up and down quark masses are then extracted by using the π^+ mass as input, whereas the strange-quark mass can be obtained from the (nonexistent) $s\bar{s}$ pseudoscalar meson whose experimental mass can be estimated from

$$m_{s\bar{s}}^2 = 2m_{K^+}^2 - m_{\pi^+}^2$$

to be around 686 MeV. Similar estimates can be alternatively obtained by using the ϕ -meson mass as input. Thus at the different values of β we get the following series of estimates for the ρ mass in lattice units, the inverse lattice spacing, the ratio of pseudoscalar mass squared over quark mass in lattice units, the sum of up and down quark masses and the strange-quark mass, and the pion decay constant:

β	am_{ρ}	a^{-1} (MeV)	am_P^2/m	$m_u + m_d$ (MeV)	m_s (MeV)	f_{π} (MeV)
5.6	0.78	970	6.3	6.4	75	175
5.7	0.75	1010	6.2	6.3	75	155
5.8	0.61	1210	5.4	6.0	70	170
5.9	0.54	1410	4.4	6.3	75	160
6.0	0.45	1690	3.4	6.8	80	140

The results would lead us to conclude that although the numbers in lattice units change significantly in the region of β explored, when they are reexpressed in physical units little change is observed as the gauge coupling is reduced. In Fig. 5 we have plotted the ρ mass as a function of β to show the approximate scaling behavior observed in this region. Again, as in the case of $\langle \bar{\psi}\psi \rangle$, it appears that the ρ mass in lattice units decrease slightly more rapidly than asymptotic freedom would predict.

From our analysis on the $8 \times 8 \times 8 \times 16$ lattice at $g^2 \approx 1$ we arrive at the estimates for the bare quark masses and the lattice pion decay constant

$$m_u + m_d = 6.4 \pm 1.0 \text{ MeV}, \quad m_s = 75 \pm 9 \text{ MeV}, \quad (3.14)$$

$$f_{\pi} = 160 \pm 16 \text{ MeV}.$$

TABLE VIII. The mass of the first radial excitation of the pseudoscalar meson as a function of β and m obtained on the $8 \times 8 \times 8 \times 16$ lattice. The numbers in parentheses indicate the error.

$\beta \backslash m$	0.30	0.25	0.20	0.15	0.10	0.05	0.00
5.6	1.47(5)	1.36(4)	1.26(8)	1.20(4)	1.05(4)	0.92(5)	0.75
5.7	1.51(5)	1.39(7)	1.35(12)	1.20(16)	1.14(9)	1.02(14)	0.88
5.8	1.54(12)	1.42(12)	1.39(6)	1.30(14)	1.20(10)	1.09(23)	0.96
5.9	1.55(5)	1.50(19)	1.42(11)	1.30(5)	1.25(17)	1.10(13)	1.00
6.0	1.50(9)	1.44(14)	1.38(6)	1.32(5)	1.20(4)	1.17(5)	1.10

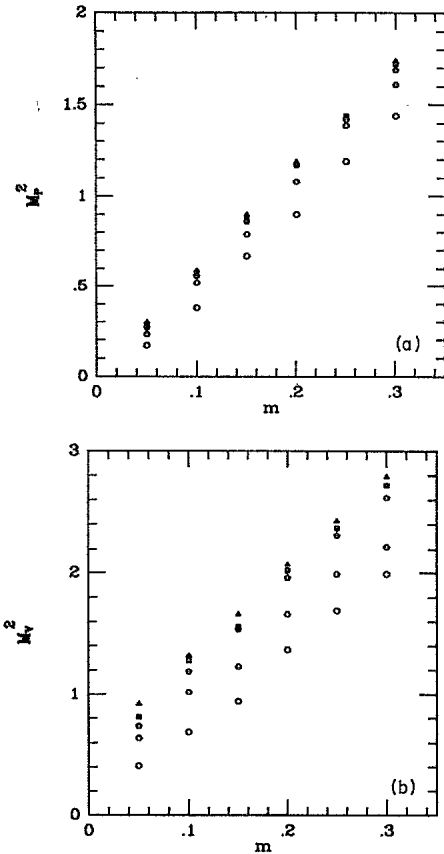


FIG. 4. (a) Pseudoscalar- and (b) vector-meson masses squared as a function of the quark mass and the gauge coupling constant: $\beta=5.6$ (triangles), $\beta=5.7$ (squares), $\beta=5.8$ (pentagons), $\beta=5.9$ (hexagons), and $\beta=6.0$ (circles).

From the vector-meson mass (by using the ϕ meson as input) we would have obtained the slightly less accurate estimate $m_s = 66 \pm 15$ MeV.

We have quoted here the bare quark masses at $g^2 \approx 1$, and it is unclear what the corresponding momentum scale is. The renormalization-group-invariant masses \bar{m} were defined in Refs. 5 and 6 through

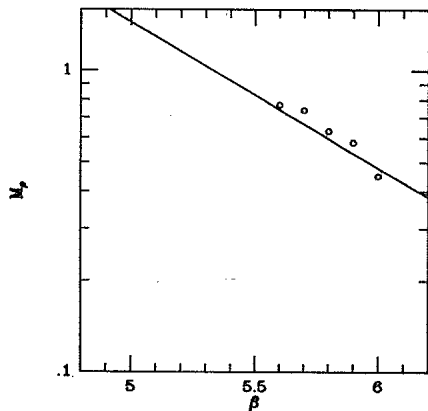


FIG. 5. The ρ mass as a function of β . The expected renormalization-group behavior is also shown and the straight line represents the estimate $m_\rho = (205 \pm 20) \Lambda_{\text{latt}}$.

$$\bar{m} = \left[3 \frac{g^2}{4\pi} \right]^{-4/11} m(a), \quad (3.15)$$

where m is the bar quark mass. Some care is needed when comparing the quark masses on the lattice with the quark masses in the continuum, because of perturbatively computable finite-renormalization effects that can be significant in the presently accessible coupling-constant region. The relationship between the bare quark mass on the lattice $m(a)$ and the invariant quark mass \bar{m} in the modified minimal-subtraction ($\overline{\text{MS}}$) scheme is given for SU(3) and $n_f=0$ by the formula¹⁶

$$\bar{m} = \left[\frac{2\pi}{9} \left[\beta + \frac{33}{4\pi^2} \ln \frac{\Lambda_{\overline{\text{MS}}}}{\Lambda_{\text{latt}}} + \frac{33}{4\pi^2} \ln C_m \right] \right]^{4/11} m(a). \quad (3.16)$$

One has that $\ln C_m = 6.53$ for $r=0$ and $\Lambda_{\text{latt}}/\Lambda_{\overline{\text{MS}}} = 24.5$, and therefore $\bar{m} \approx 1.92 m(a)$ in the region considered here. The estimates for the invariant masses then become $\bar{m}_u + \bar{m}_d = 12.2 \pm 2.0$ MeV and $\bar{m}_s = 145 \pm 20$ MeV, a more reasonable set of values.

For the pion decay constant, taking into account the perturbative correction factor of Eq. (3.9), we then get that f_π in the continuum is about 140 ± 15 MeV, which should be compared to the experimental value of 93.5 MeV. This high value is not surprising given the high value of the pion decay constant at strong coupling, the presence of perturbative corrections to lattice current matrix elements and the sensitivity of the pion wave function (more than its mass) to the coarseness of the lattice. It is known that the estimates for the hadron masses do not have any correction factors proportional to g^2 (the corrections are of order $a^2 \Lambda^2$ for weak coupling), and thus are likely to be more accurate. On the other hand, one can see that there is clearly a trend towards lower values of f_π as the gauge coupling is decreased.

It would appear that some of our results do not agree with the analogous quantities in the Wilson fermion case. This is not surprising since the two-fermion action becomes equivalent only in the continuum limit, i.e., for small g^2 . In fact it is known that at strong coupling some quantities, like the ρ mass in lattice units and therefore the lattice spacing, can differ by as much as a factor of 2.

Still we notice that a substantial deviation from the strong-coupling values has taken place. In fact at $g^2 N_c = \infty$ one has for Susskind fermions $am_\rho = 1.76$ and therefore $a^{-1} = 430$ MeV from which one obtains $m_u + m_d = 20.1$ MeV, $m_s = 241$ MeV, and $f_\pi = 201$ MeV. It is also of interest to see the amount of deviation from the PCAC (partial conservation of axial-vector current) formula (3.11). On the lattice we have shown that for Euclidean Susskind fermions the PCAC relationship is exactly satisfied for the pion of Eq. (3.8). As a check on our numerical results we have computed the ratio

$$\frac{2f_P^2 m_P^2}{m \langle \bar{\chi} \chi \rangle}, \quad (3.17)$$

which one expects to approach the value 1 for small m . At $\beta=5.6, 5.7, 5.8, 5.9$, and 6.0 we find for the ratio the values $0.84, 0.61, 1.33, 1.08$, and 0.67 , respectively, which give on the average 0.90 . Thus it appears that the PCAC relation is satisfied within the errors.

IV. RENORMALIZATION-GROUP ANALYSIS

In this section we continue to discuss the dependence of our results on the infrared cutoff arising due to the finite spatial extent of the box. A real-space renormalization-group transformation can be constructed from the requirement that physical quantities be invariant under a change of the linear size of the system size. In our discussion here we will borrow from a set of ideas on finite-size scaling properties of thermodynamic functions due originally to Fisher and collaborators¹⁷ and later elaborated by others.¹⁸ In Ref. 3 it was suggested that these studies may elucidate further the significance for the infinite system of results obtained on small lattices. By using these methods one hopes to extract as much information as possible about the infinite system by analyzing a sequence of small finite-size systems.

Here we will restrict our discussion to a geometry in which the size of the system is $L \times L \times L \times T$ with $T \rightarrow \infty$. Now consider an observable (like a physical mass) $F_L(g)$ on a finite lattice and assume an algebraic singularity close to the critical point $F_\infty(g) \sim A(g-g_c)^\omega$ for $g \rightarrow g_c$. Denoting by ξ_∞ the correlation length (the inverse of the mass gap) in the infinite system, then on a finite lattice one expects that for $\xi, L \gg a$,

$$\frac{F_L(g)}{F_\infty(g)} = f\left(\frac{L}{\xi_\infty}\right) \quad (4.1)$$

with $f(x)$ a universal function dependent on F and the boundary conditions. Since one knows that $f(x) \rightarrow 1$ for $x \rightarrow \infty$ and $f(x) \rightarrow cx^{-\omega/\nu}$ for $x \rightarrow 0$, this suggests that F_L should have the scaling form

$$F_L(g) = L^{-\omega/\nu} h(Lt^\nu), \quad (4.2)$$

where we have set $t = (g-g_c)/g_c$. The validity of this form can be demonstrated in the $\lambda\phi^4$ theory where for $a \rightarrow 0$ physical observables like N -point functions for finite L obey the same renormalization-group equations as for infinite L . Define μ to be the renormalization point and $t = (T-T_c)/T_c$. Then this implies that the ratio

$$\phi_L(\mu, t, \lambda) = \frac{F_L}{F_\infty} \quad (4.3)$$

obeys the equation

$$\left[\mu \frac{\partial}{\partial \mu} + \beta(\lambda) \frac{\partial}{\partial \lambda} + \gamma(\lambda) t \frac{\partial}{\partial t} \right] \phi_L(\mu, t, \lambda) = 0. \quad (4.4)$$

As a consequence one then obtains from the usual scaling arguments for $L\mu \gg 1$

$$\phi_L(\mu, t, \lambda) = \phi_1(1, tL^{1/\nu}, \lambda^*) \quad (4.5)$$

and it has been tacitly assumed that λ^* , the value of the running coupling constant at the infrared fixed point, is nonvanishing. For $\lambda\phi^4$ this is indeed true below four dimensions. At four dimensions one expects logarithmic corrections to scaling, whose form can be computed exactly in the N -vector model for large N (Ref. 19). In the case of lattice QCD the bare gauge coupling g plays the role of t and the argument of the scaling functions has a different form: for a physical mass one has that the quantity Lt^ν is replaced by $L \exp[-1/2(\beta_0 g^2)]$.

An important consequence of the property stated in Eq. (4.1) is that it allows one to construct a renormalization-group transformation which is exact for $\xi_\infty L \gg a$ and calculable on a finite system. Define a scale transformation $L \rightarrow L'$ and $g \rightarrow g'$ such that

$$LM_\infty(g) = L'M_\infty(g') \quad (4.6)$$

holds. The masses in the infinite system are usually unknown, but can be eliminated by realizing that (4.1) and (4.6) imply

$$\frac{M_L(g)}{M_\infty(g)} = \frac{M_{L'}(g')}{M_\infty(g')}, \quad (4.7)$$

which gives for the final form of the renormalization-group transformation

$$LM_L(g) = L'M_{L'}(g'). \quad (4.8)$$

For weak-enough gauge coupling the amount by which g has to be changed under a scale transformation $L \rightarrow L'$ is known. At one-loop order one has

$$\frac{1}{g'^2} = \frac{1}{g^2} + 2\beta_0 \ln \frac{L'}{L}. \quad (4.9)$$

At two-loop order one can define the change in g^2 to be such that the ratio of sizes L/L' is equal to the ratio of lattice Λ parameters Λ'/Λ .

In principle $M(g)$ can be any physical mass. We have chosen as our physical observable the ρ mass, since it can be determined more accurately than the glueball mass, whose correlation function is usually difficult to measure for large separation because of statistical noise. The renormalization of the coupling constant was determined by comparing results for m_ρ on the $8 \times 8 \times 8 \times 16$ lattice with results on a $4 \times 4 \times 4 \times 16$ lattice. For one value of the coupling we also used previously obtained results on a $6 \times 6 \times 6 \times 12$ lattice. The ρ mass on the $L=4$ lattice was obtained by computing the pseudoscalar- and vector-meson mass m_P and m_V for $m=0.3, 0.2$, and 0.1 on two gauge configurations for each β and linearly extrapolating then $m_V^2 - m_P^2$ to $m=0$. We have chosen the lattice to be significantly longer in the time direction so as to allow us to determine as accurately as possible the true energy-level splitting on the spatially finite lattice. As a consequence our results are more sensible to the infrared cutoff and less sensible to the short-distance features. In Fig. 6(a) we show the quantities $Lm_L(g)$ as a function of $1/g^2$ for $L=4$ and $L=8$. In two limits the expected behavior of this quantity is known:

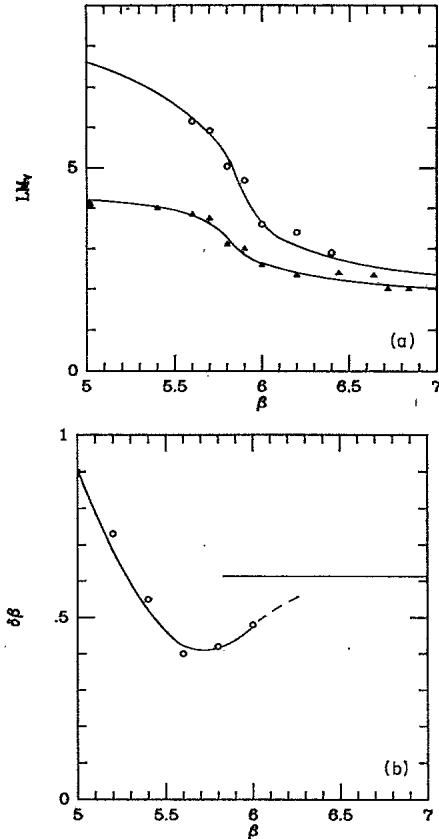


FIG. 6. (a) The ρ mass on a finite lattice times the linear spatial extent of the lattice Lm_L as a function of β for $L=4$ (lower curve) and $L=8$ (upper curve). (b) The shift in the coupling β necessary to have the two curves in the preceding figure overlap. The almost horizontal line shows the two-loop perturbative behavior expected at large β .

$$Lm_L \rightarrow L \cosh^{-1} 3 \quad (g^2 \rightarrow \infty),$$

$$Lm_L \rightarrow \text{constant} \quad (g^2 \rightarrow 0),$$
(4.10)

and our results are consistent with these results. Note that an intersection of the two curves (for $L=4$ and $L=8$) would indicate the presence of a phase transition. On the other hand, asymptotic-freedom scaling predicts that the distance between the two curves should become independent of g^2 for small enough g^2 . In other words, a finite shift of one of the two curves should make them overlap. In Fig. 6(b) we show the shift $\delta\beta$ in β that would be required to have the values of Lm_L on the two lattices with $L=4$ and $L=8$ match. Taking into account two-loop corrections one would expect that in the region $6.0 < \beta < 7.0$ the shift should be about $\delta\beta = 0.61$. It appears from the graph that there is a tendency to overshoot the asymptotic-freedom prediction and that the correct answer might be recovered only for values of β larger than 6.0.

Several comments are in order. It is clear that the statistics and the number of data points are not at the moment sufficient to reach any definite conclusion, especially for weaker gauge coupling. It also would be extremely helpful to have results on larger lattices such as

$12 \times 12 \times 12 \times 32$ and $16 \times 16 \times 16 \times 32$. In particular, for $L=4$ it is unclear that one is in a regime where $L \gg a$. We are now improving on the statistics and will present the results elsewhere. Still it appears that the methods that we have presented can be used to shed more light on the region $g^2 < 1$, and the way by which the lattice results match onto the weak-coupling scaling predictions.

V. CONCLUSIONS

In the previous sections we have presented new and more accurate results for $\langle \bar{\psi}\psi \rangle$ and light-meson and quark masses and compared the results to previous calculations. The new estimates appear to be consistent with the old ones, given the lower statistics and larger errors of the previous results. Still it appears that studies on larger lattices and with even better statistics are important and should be performed to check all the results and fully determine the size and significance of systematic errors due to the finite box size, quark mass, and gauge coupling constant.

Note added. After this work was completed, papers²⁰ appeared in which similar results for the fermion condensate $\langle \bar{\psi}\psi \rangle$ and the π and ρ mass in lattice QCD with Susskind fermions are presented. The lattice size ($8^3 \times 16$ and $10^3 \times 16$) and the number of gauge configurations used is comparable to the present study. While there is general agreement in the values of the chiral condensate, there appears to be some rather significant discrepancy in the results for the π and ρ masses. These are in the quoted papers always significantly higher than the present estimates at finite- and zero-quark mass. The reason for this discrepancy should be ascribed to the fact that the quark and meson propagators are evaluated there at too small quark masses (m equal or less than 0.05 in lattice units). This circumstance makes it difficult to evaluate the true asymptotic behavior of the propagator at large time separations and introduces large systematic errors in the meson masses. Their final estimates for the π and ρ mass, the pion decay constant, and the quark masses are therefore also likely to be affected by large systematic errors.

For the above reasons the extrapolation to small quark mass by using six larger values of the same was preferred in this paper. The problems of extrapolation mentioned above have been previously extensively discussed in the literature (see, for example, Refs. 3, 5, and 6). It should be pointed out that the results presented in this paper for the π and ρ mass appear to be in good agreement with the recent results of Ref. 21 at $\beta=5.7$ on a similar size lattice.

ACKNOWLEDGMENTS

I wish to thank Giorgio Parisi for clarifying discussions at the Cargèse Summer School. I also thank the Colliding Beam Accelerator at BNL for the use of their VAX in the early stages of this work, and the National Magnetic Fusion Energy computer center at the Lawrence Livermore Laboratory for use of three hours of their Cray 1s. This research was supported by the U.S. Department of Energy under Grant No. DE-AC02-76ER02220.

- ¹K. G. Wilson, *Phys. Rev. D* **10**, 2445 (1974); in *New Phenomena in Subnuclear Physics*, proceedings of the 14th Course of the International School of Subnuclear Physics, Erice, 1975, edited by A. Zichichi (Plenum, New York, 1977).
- ²K. G. Wilson, in *Recent Developments in Gauge Theories*, proceedings of the NATO Advanced Study Institute, Cargèse, 1979, edited by G. 't. Hooft (Plenum, New York, 1980).
- ³H. Hamber, in *Proceedings of the VIIth International Congress on Mathematical Physics, Boulder, Colorado*, edited by W. E. Brittin *et al.* [Physica (Utrecht) **124A**, 365 (1984)].
- ⁴K. Symanzik, in *Mathematical Problems in Theoretical Physics*, (Lecture Notes in Physics, Vol. 153), edited by R. Schrader *et al.* (Springer, Berlin, 1982); DESY Reports Nos. 83-016, 83-026, 1983 (unpublished); P. Weisz, *Nucl. Phys.* **B212**, 485 (1983).
- ⁵H. Hamber and G. Parisi, *Phys. Rev. Lett.* **47**, 1792 (1981).
- ⁶H. Hamber and G. Parisi, *Phys. Rev. D* **27**, 208 (1983).
- ⁷N. Kawamoto, *Nucl. Phys.* **B190** [FS3], 617 (1981); N. Kawamoto and J. Smit, *ibid.* **B192**, 100 (1982); J. Hoek, N. Kawamoto, and J. Smit, *ibid.* **B199**, 495 (1982).
- ⁸J. Kogut and L. Susskind, *Phys. Rev. D* **11**, 395 (1975); L. Susskind, *ibid.* **16**, 3031 (1977).
- ⁹J. M. Blairon, R. Brout, F. Englert, and J. Greensite, *Nucl. Phys.* **B180** [FS2], 439 (1981).
- ¹⁰H. Kluberg-Stern, A. Morel, O. Napoly, and B. Peterson, *Nucl. Phys.* **B190** [FS3], 504 (1981); *Phys. Lett.* **114B**, 152 (1982); *Nucl. Phys.* **B220**, 447 (1983).
- ¹¹E. Marinari, G. Parisi, and C. Rebbi, *Phys. Rev. Lett.* **47**, 1795 (1981); see also J. Kogut *et al.*, *ibid.* **48**, 1140 (1982); **50**, 393 (1983); University of Illinois Report No. ILL (TH) 83-9, 1983 (unpublished).
- ¹²G. Parisi, *Nucl. Phys.* **B180** [FS2], 378 (1981); **B205** [FS5], 337 (1982).
- ¹³M. Creutz, *Phys. Rev. D* **21**, 2308 (1980); *Phys. Rev. Lett.* **45**, 313 (1980); E. Pietarinen, *Nucl. Phys.* **B190** [FS3], 349 (1981).
- ¹⁴M. Creutz and K. Moriarty, *Phys. Rev. D* **26**, 2166 (1982); R. Ardill, M. Creutz, and K. Moriarty, *ibid.* **27**, 1956 (1983); M. Fukugita, T. Kaneko, and A. Ukawa, *ibid.* **28**, 2696 (1983); F. Gutbrod, P. Hasenfratz, Z. Kunszt, and I. Montvay, *Phys. Lett.* **128B**, 415 (1983).
- ¹⁵B. Meyer and C. Smith, *Phys. Lett.* **123B**, 62 (1982); G. Martinelli and Y. C. Zhang, *ibid.* **123B**, 433 (1983); R. Groot, J. Hoek, and J. Smit, *Nucl. Phys.* **B237**, 111 (1984).
- ¹⁶A. Gonzales-Arroyo, G. Martinelli, and F. Yndurain, *Phys. Lett.* **117B**, 437 (1982); **122B**, 486(E) (1983); H. Hamber and C. M. Wu, *ibid.* **133B**, 351 (1983).
- ¹⁷M. E. Fisher and A. E. Ferdinand, *Phys. Rev. Lett.* **19**, 169 (1967); M. E. Fisher and M. Barber, *ibid.* **28**, 1516 (1972); *Ann. Phys. (N.Y.)* **77**, 1 (1973).
- ¹⁸M. Nightingale, *Physica (Utrecht)* **83**, A561 (1976); B. Derri-da, *J. Phys. A* **14**, L5 (1981); C. Hamer and M. Barber, *J. Phys. B* **13**, L169 (1980); V. Privman and M. E. Fisher, *J. Phys. A* **16**, L295 (1983), and references therein.
- ¹⁹E. Brezin, *Ann. Phys. (Paris)* (to be published).
- ²⁰I. M. Barbour *et al.*, *Phys. Lett.* **136B**, 80 (1984); **136B**, 87 (1984); DESY Report No. 84-021 (unpublished).
- ²¹R. C. Bowler *et al.*, Edinburgh Report No. 84-295 (unpublished).